Orthopaedic Surgery

SCIENTIFIC ARTICLE

Biomechanical Study on the Stress Distribution of the Knee Joint After Tibial Fracture Malunion with Residual Varus–Valgus Deformity

Ming Li, MD[1†], Hengrui Chang, MD[2†], Ning Wei, MD[3], Wenli Chang, MD[4], Ying Yan, MD[1], Zeyue Jin, MD[1], Wei Chen, MD[1,5]

Department of [1]Orthopedic Surgery and [2]Spine Surgery, The Third Hospital of Hebei Medical University, [3]Department of Orthopedic Surgery, The Fourth Hospital of Shijiazhuang and [5]Key Laboratory of Biomechanics of Hebei Province, Shijiazhuang and [4]Department of Orthopedic Surgery, Cangzhou Hospital of Integrated TCM-WM Hebei, Cangzhou, China

Objective: To investigate the effect of residual varus and valgus deformity on the stress distribution of the knee joint after tibial fracture malunion.

Methods: Fourteen adult cadaver specimens were selected to establish the models of tibial fractures, which were fixed subsequently at neutral position (anatomical reduction) and malunion positions (at 5°, 10°, and 15° valgus positions, and 5°, 10°, and 15° varus positions). The stress distribution on the medial and lateral plateau of the tibia was quantitatively measured using ultra-low-pressure sensitive film technology. The changes in the stress distribution of the knee joint after tibial fracture malunion and the relationship between the stress values and the residual varus or valgus deformity were analyzed.

Results: Under 400 N vertical load, the stress values on the medial and lateral plateau of the tibia at the neutral position were 1.137 ± 0.139 MPa and 1.041 ± 0.117 MPa, respectively. When compared with the stress values measured at the neutral position, the stress on the medial plateau of the tibia was significantly higher at varus deformities and lower at valgus deformities, and the stress on the lateral plateau was significantly higher at valgus deformities and lower at varus deformities (all $P < 0.05$). The stress values on the medial plateau of the tibia were significantly higher than the corresponding data on the lateral plateau at neutral and 5°, 10°, and 15° varus deformities, respectively (all $P < 0.05$), and significantly lower than the corresponding data on the lateral plateau at 5°, 10°, and 15° valgus deformities, respectively (all $P < 0.05$).

Conclusion: Residual varus and valgus deformity after tibial fracture malunion can lead to obvious changes of the stress distribution of the knee joint. Therefore, tibial fractures should be reduced anatomically and fixed rigidly to avoid residual varus–valgus deformity and malalignment of lower limbs.

Key words: Biomechanics; Knee joint; Malunion; Tibia fracture; Valgus deformity; Varus deformity

Introduction

The incidence of proximal tibial fractures due to high-energy trauma has increased gradually, today accounting for 5%–11% of all tibial fractures[1–3]. Surgical treatment of these traumas remains a major clinical challenge[4–6], and functional recovery is affected by various factors, including

Address for correspondence Wei Chen, MD, Department of Orthopedic Surgery, The Third Hospital of Hebei Medical University, No. 139 Ziqiang Road, Qiaoxi District, Shijiazhuang, China 050051 Tel: +86 18533112839; Fax: +86 311 87023626; Email: drchenwei1@163.com
†These authors contributed equally to this work.
Grant Sources: This study was supported by the National Natural Science Foundation of China (Grant No. 81401789) and Hebei National Science Foundation-Outstanding Youth Foundation (Grand No. H2017206104).
Disclosure: This study has been reviewed and approved by the Institutional Review Board (IRB) of the Third Hospital of Hebei Medical University. This study was supported by the National Natural Science Foundation of China (Grant No. 81401789) and the Hebei National Science Foundation-Outstanding Youth Foundation (Grand No. H2017206104).
Received 29 January 2020; accepted 11 March 2020

the injury mechanism, the severity of the initial injury, treatment options, and the quality of fracture reduction. Although continuous advances in internal fixation devices and surgical techniques have improved the therapeutic effect of tibial fractures, malunion of the proximal tibia fracture and malalignment of lower extremities still occur[7,8]. Greenwood *et al.*[9] compared 398 tibia fracture patients with 1573 age-matched and gender-matched populations and found that the incidence of knee pain and dysfunction in the fracture group was significantly higher than that in the control group. Malunion of fractures can disrupt normal joint movement, leading to non-physiological stress and traumatic arthritis (TA) of the knee[10,11]. Malunion and malalignment of lower limbs after fracture healing is an important factor for knee and ankle joints to develop TA. Studies show that an individual with tibial fractures that heal with residual deformity may have increased risk of pain and stiffness in knee and ankle joints[12].

To identify the pathogenesis of traumatic arthritis and the effects of different interventions for traumatic fractures of lower extremities, some scholars have conducted research using techniques including imaging, biomechanics, and finite element analysis[13–15]. Kettelkamp *et al.*[16] conducted a long-term follow-up study of patients with femoral shaft fractures, and found that knee TA with obvious local symptoms can occur after 32 years due to residual deformity and long-term weight-bearing. Patients with previous knee fractures who have severe arthritis and need total knee arthroplasty are not uncommon. Accordingly, improved biomechanical understanding of tibial varus or valgus malunions will help to formulate improved treatment algorithms.

Therefore, a biomechanical study was conducted using the cadaver models of middle and upper tibial fractures. The fractures were fixed at different varus and valgus deformities, and the stress distribution on the medial and lateral plateau of the tibia under weight-bearing load were measured. The purpose of the present study was to: (i) investigate the changes of the stress on the medial and lateral plateaus after tibial fracture malunion through comparison with normal stress; (ii) identify the relationship between the stress on the plateaus and the residual varus or valgus deformity; and (iii) highlight to the surgeon the importance of reducing the risk of residual varus and valgus deformity during the treatment of tibial fractures.

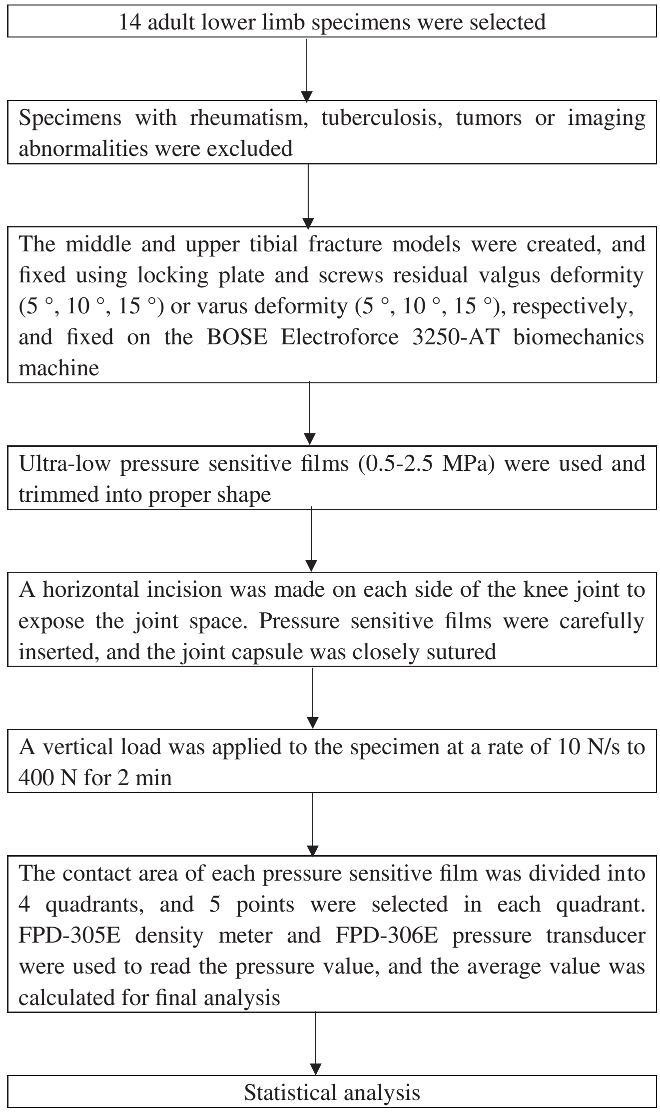

Fig. 1 The experimental flowchart of the biomechanical study illustrated the main procedures, including specimen preparation, establishment of tibial fracture and malunion models, assembly of specimens on the biomechanical testing machine, ultra-low-pressure sensitive film preparation, stress measurement and read, data collection, and statistical analysis.

Materials and Methods

The present study has been reviewed and approved by the Institutional Review Board (IRB) of the Third Hospital of Hebei Medical University. The experimental flowchart of this biomechanical study is presented in Fig. 1.

Specimen Preparation

Fourteen formalin-soaked specimens were all from adult male donated bodies. The body height of the specimens was 171 cm on average (range, from 163 to 181 cm). The age when donated was 55 years on average (range, from 42 to 65 years old). Samples from those who had rheumatism, tuberculosis, or tumors were excluded. The specimens were examined with digital radiography and excluded if they were identified to have osteoporosis, pathological or anatomical deformity, irregular joint surface, or other imaging abnormalities. All samples were required to have intact ligaments and tendons around the knee joint and an unbroken joint capsule. The muscular tissue of each specimen was removed. Then, the upper part of the femur and the distal part of the tibial and fibula were dissected. The remaining femur and tibial and fibula were both approximately 25 cm in length.

The specimens were maintained in standby packages to prevent dehydration and kept at −20°C for cryopreservation.

Establishment of Tibial Fracture Malunion Model

The cadaver specimens were thawed at room temperature for 12 hours before the experiment. The middle and upper tibial fracture models were created, and fixed using locking plates and screws at various residual valgus deformities (5°, 10°, or 15°), neutral position (0°, anatomically reduced), or varus deformities (5°, 10°, or 15°), respectively. A horizontal incision approximately 3–4 cm in length was made at the level of the joint space on each side. The subcutaneous fat was separated, the bursa was cut, and the joint space was exposed. The anterior and posterior cruciate ligaments and the medial and lateral menisci were preserved so as not to affect the normal distribution of the contact stress of the knee joint.

Specimen Assembled to Biomechanical Testing Machine

The specimen was first erected, and the femur end was fixed perpendicularly to the homemade clamp with the use of denture base resin and solution (type II self-setting dental powder and tray water). After the dental powder and tray water solidified, the tibial end of the specimen was fixed in the same way. Then the two-ends of the clamp were assembled to the biomechanical testing machine (Electroforce 3520-AT, Bose company, USA), and the fixed position of the femoral and tibia stumps was adjusted so that the lower limb mechanical axis was close to the position when standing naturally (Fig. 2).

Stress Measurement and Data Collection

An ultra-low-pressure sensitive film (0.5–2.5 MPa) was used to measure the contact pressure on the medial and lateral plateaus of the tibia. The pressure sensitive film was trimmed to a suitable shape and sealed in a polyethylene film bag. The total thickness of the pressure sensitive film and the polyethylene film bag was controlled to 250 μm. The pressure sensitive films were carefully placed under the knee meniscus[15] separately through the medial and lateral incisions (Fig. 3). The incisions were then sutured tightly to close the joint capsule. After stabilization, the specimen was pressurized to 200 N at 10 N/s to eliminate creep. A vertical load was applied on the specimen at a rate of 10 N/s to 400 N for 2 min. Then, the pressure sensitive film was carefully removed from the knee joint.

The stress values of the ultra-low-pressure sensitive films were read with the use of an FPD-305E densitometer and an FPD-306E pressure transducer (Fuji Company, Japan). The contact area of each pressure sensitive film was divided into four quadrants (front outer, front inner, rear inner, and rear outer). Five points were selected in each quadrant for stress value reading. A total of 20 values in each film were recorded and the average was calculated for final analysis.

Fig. 2 The specimens were assembled to the BOSE Electroforce 3520-AT biomechanical testing machine, and the position of the femoral and tibia stumps was adjusted so that the lower limb mechanical axis was close to the position when standing naturally.

Statistical Analysis

SPSS 21.0 software (SPSS, Chicago, IL, USA) was applied for statistical analysis. The variables in this study include stress values and angles of varus or valgus deformity. The normality of the stress data is verified using the Shapiro–Wilk test, and the variance consistency was verified using the Levene test. Normally distributed measurement data was recorded as mean ± standard deviation. The stress values on the medial and lateral plateau of the tibia at different positions were calculated and recorded, respectively. Analysis of variance (ANOVA) for random block groups was used to compare

Fig. 3 The ultra-low-pressure sensitive films were carefully placed under the knee meniscus separately through the medial and lateral incisions.

the stress values on the medial or lateral plateau at different angles of tibia varus or valgus deformity under vertical load. The Student–Newman–Keuls test was applied to make pairwise comparisons between the multiple sample measurements. Differences in the stress data between medial and lateral plateaus were tested using the paired samples *t* test. A *P*-value less than 0.05 indicated a statistically significant difference.

Results

Stress Distribution on the Medial Plateau of the Tibia Measured at Different Varus and Valgus Deformities

The stress values on the medial plateau of the tibia measured at different varus and valgus deformities under 400 N vertical load are summarized in Table 1. ANOVA for random block groups revealed statistically significant differences in the stress values on the medial plateau among different varus and valgus deformities (including the neutral position) ($F = 304.097$, $P < 0.001$). The Student–Newman–Keuls test revealed statistically significant differences in the stress values on the medial plateau between pairwise comparisons among 15°, 10° and 5° varus deformities, the neutral position (0°), and 5°, 10° and 15° valgus deformities. The stress values on the medial plateau measured at 5°, 10°, and 15° varus deformities were significantly higher than that measured at neutral position (all $P < 0.05$). In contrast, the stress values on the medial plateau measured at 5°, 10°, and 15° valgus deformities were significantly lower than that measured at neutral position (all $P < 0.05$). From 15° of valgus deformity to 15° of varus deformity, the stress values on the medial plateau of the tibia increased proportionably (Fig. 4).

Stress Distribution on the Lateral Plateau of the Tibia Measured at Different Varus and Valgus Deformities

The stress values on the lateral plateau of the tibia measured at different varus and valgus deformities under 400 N vertical load are recorded and summarized (Table 1). ANOVA for random block groups revealed statistically significant differences in the stress values on the lateral plateau among different varus and valgus deformities (including the neutral position) ($F = 668.663$, $P < 0.001$). There were statistically significant differences between pairwise comparisons among 15°, 10° and 5° varus deformities, neutral position, and 5°,

TABLE 1 The stress values (Mpa) on the medial and lateral plateau of the tibia measured on the models of different varus and valgus deformities under 400 N vertical load

Deformity angle	Medial plateau (n = 14)	Lateral plateau (n = 14)	*t*-value	*P*-value
Valgus 15°	0.814 ± 0.120	1.436 ± 0.094	−15.25	<0.001*
Valgus 10°	0.925 ± 0.140	1.318 ± 0.089	−8.873	<0.001*
Valgus 5°	1.031 ± 0.152	1.190 ± 0.108	−3.186	0.004*
Neutral position (0°)	1.137 ± 0.139	1.041 ± 0.117	−1.973	0.045*
Varus 5°	1.255 ± 0.115	0.937 ± 0.103	7.705	<0.001*
Varus 10°	1.372 ± 0.110	0.829 ± 0.115	12.81	<0.001*
Varus 15°	1.489 ± 0.097	0.715 ± 0.115	19.25	<0.001*
F-value	304.097	668.663	—	—
P-value	<0.001†	<0.001‡	—	—

* Comparison of differences in the stress data between medial and lateral plateau of the tibia at different deformed angles.; † Comparison of differences in the stress data on the medial plateau of the tibia at different deformed angle.; ‡ Comparison of differences in the stress data on the lateral plateau of the tibia at different deformed angle.

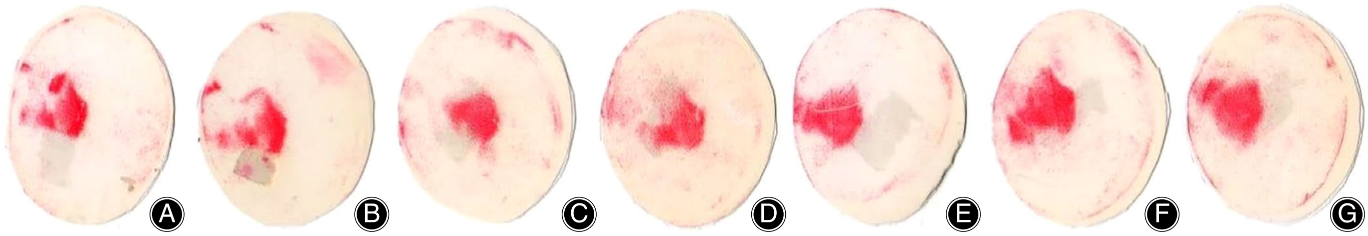

Fig. 4 Color changes of the ultra-low-pressure sensitive films measured on the medial plateau at different angles of varus and valgus deformities of the tibia: (A) valgus 15°; (B) valgus 10°; (C) valgus 5°; (D) neutral position 0°; (E) varus 5°; (F) varus 10°; and (G) varus 15°.

10° and 15° valgus deformities according to the Student–Newman–Keuls test. The stress values on the lateral plateau measured at 5°, 10°, and 15° valgus deformities were significantly higher than that measured at neutral position (all $P < 0.05$). Conversely, the stress values on the lateral plateau measured at 5°, 10°, and 15° varus deformities were significantly lower than that measured at neutral position (all $P < 0.05$). From 15° of valgus deformity to 15° of varus deformity, the stress values on the lateral plateau of the tibia decreased proportionably (Fig. 5).

Comparison of the Stress Values Between Medial and Lateral Plateaus of the Tibia

Under 400 N vertical load, the stress on the medial plateau of the tibia was 1.137 ± 0.139 MPa at the neutral position, which was significantly higher than the value of 1.041 ± 0.117 MPa on the lateral plateau of the tibia ($P < 0.05$). Under 400 N vertical load, the stress values on the medial plateau of the tibia were significantly higher than the corresponding values on the lateral plateau at 5°, 10°, and 15° varus deformity positions in addition to neutral position, respectively (all $P < 0.05$), and significantly lower than the corresponding values on the lateral plateau at 5°, 10°, and 15° valgus deformity positions, respectively (all $P < 0.05$).

Discussion

Tibial fractures are common injuries in traumatic orthopaedics. Open or closed reduction and internal fixation are the standard treatment options for displaced tibial fractures. However, during closed reduction and intramedullary nailing, fractures cannot always be reduced anatomically, and various residual fracture deformities and complications may occur. In Milner (2002)[17], 47 (29%) patients with tibial shaft fractures were found to have an angular deformity of more than 5° in the coronal plane of the tibia after the operation. The change in the mechanical axis of the lower limbs after fracture malunion can lead to changes in the tension of the ligaments and joint capsules, and patella malacia in the long term. If not corrected in time, this can affect the biomechanical characteristics of knee and ankle joints and, ultimately, result in TA, followed by impaired knee function. Van der Schoot *et al.*[18] found that 20% (18/88) of patients with malunion of tibial fractures had symptoms of arthritis of the knee and ankle joints in the affected lower extremities. Studies have suggested that degenerative changes of the knee joint due to malalignment of the mechanical axis of lower extremities are directly related to the unreasonable distribution of stress in the joint[19,20]. Therefore, malunion and malalignment of the lower limb is an important factor contributing to traumatic arthritis of the knee joint.

Alignment of the lower limb is a prerequisite for ensuring a reasonable distribution of joint stress. Under normal conditions, the lower limb mechanical axis is from the center of the hip joint to the center of the ankle joint, passing through the center of the knee joint, so that the load and stress on the knee joint can be reasonably dispersed[21]. When malunion and malalignment occurs after a tibial fracture, the contact characteristics of the knee joint will be altered. However, no quantitative studies were found in the literature that investigate the changes of the stress on the medial and lateral plateaus after tibial fracture malunion and explore the

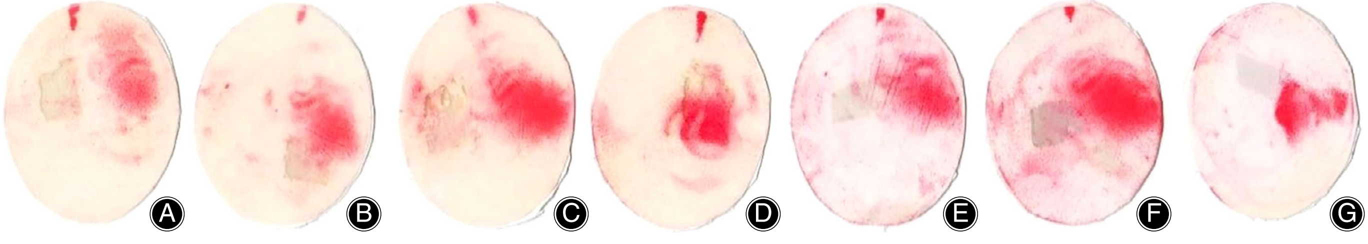

Fig. 5 Color changes of the ultra-low-pressure sensitive films measured on the lateral plateau at different angles of varus and valgus deformities of the tibia: (A) valgus 15°; (B) valgus 10°; (C) valgus 5°; (D) neutral position 0°; (E) varus 5°; (F) varus 10°; and (G) varus 15°.

relationship between the stress distribution and the residual varus or valgus deformity. Therefore, we conducted this biomechanical study on the stress distribution of the knee joint. In the current study, the malunion of proximal tibial fractures was established to simulate the varus and valgus deformities. The stress on the medial and lateral plateau of the tibia was measured on both normal and deformed knee joints using the pressure sensitive film technique. It was found that the stress on the medial and lateral plateau of the tibia changed significantly when valgus and varus deformity occurred.

In patients with knee varus deformity, the mechanical axis is offset medially from the center of the knee joint. Our findings reveal that the stress on the medial plateau of the tibia is significantly higher at varus deformities when compared with those measured at the neutral position, and significantly higher than the corresponding stress values on the lateral plateau. When the knee is at valgus position, the mechanical axis is offset laterally and the lateral compartment load increases. We also find that the stress on the lateral plateau is significantly higher at valgus deformities than the stress on the lateral plateau measured at the neutral position, as well as the corresponding data measured on the medial plateau. High stress load on the joint is an important factor causing cartilage degeneration[22]. Stress concentration will accelerate the wear of articular cartilage, stress microfracture, ischemia, and necrosis. Sharma *et al.*[23] found that the risk of knee osteoarthritis increased by 3.59 times in the medial compartment for patients with varus deformity, and the risk of knee osteoarthritis increased by 4.85 times in the lateral compartment for patients with valgus deformity. Therefore, to reduce the risk of long-term arthritis in patients, orthopaedic surgeons should reduce the fractures anatomically to avoid malalignment and malunion of lower limbs fractures[24].

In the current study, the specimen received a vertical load up to 400 N for 2 min. Ahmed *et al.*[25] applied a pressure of 890 N when measuring specimen stress on the knee joint. Riegger-Krugh *et al.*[26] selected 1960 N vertical load in the stress measurement of the knee joint, which is equivalent to three times the average body weight. Different from Ahmed and Riegger-Krugh's study, we chose 400 N vertical load applied on the single limb to simulate the static press on the knee joint of the normal body mass.

This study has some limitations. First, the sample size is small due to the limited source of specimens, which will reduce the credibility of the experimental data (type II error). Second, this study is based on cadaver specimens and cannot take the action of muscles into consideration. Third, dynamic load on the knee joint was not taken into consideration and the current model cannot simulate the stress distribution during knee motion. However, the current findings guarantee further biomechanical studies on the stress distribution of the knee joint under dynamic load, clinical studies on the quantitative relationship between residual malunion and traumatic arthritis, and the endeavor to reduce complex fractures anatomically in closed fashion or in a minimally invasive way.

In conclusion, tibial fracture malunion with residual varus or valgus deformity can lead to significant changes in the stress distribution and contact characteristics of the knee joint. Therefore, orthopaedic surgeons should reduce the fractures anatomically to avoid malunion of the fractures and malalignment of the affected lower extremities, to improve the functional recovery and reduce the risk of traumatic arthritis in the long term.

References

1. Dirschl DR, Dawson PA. Injury severity assessment in tibial plateau fractures. Clin Orthop Relat Res, 2004, 423: 85–92.
2. Rademakers MV, Kerkhoffs GM, Sierevelt IN, Raaymakers EL, Marti RK. Operative treatment of 109 tibial plateau fractures: five- to 27-year follow-up results. J Orthop Trauma, 2007, 21: 5–10.
3. Zhao DW, Ma ZJ, Wang TN, Liu BY. Biocompatible porous tantalum metal plates in the treatment of tibial fracture. Orthop Surg, 2019, 11: 325–329.
4. Toms AD, Green AL, Giles S, Thomas PB. The current management of tibial fractures: are clinical guidelines effective? Ann R Coll Surg Engl, 2003, 85: 413–416.
5. Wu WY, Xu WG, Wan CY, Fang M. Preoperative plan with 3D printing in internal and external fixation for complex tibial plateau fractures. Orthop Surg, 2019, 11: 560–568.
6. Jia P, Lu FC, Ullah K, *et al*. Angle stable interlocking intramedullary nails for tibial plateau fractures. Orthop Surg, 2018, 10: 115–120.
7. Krettek C, Miclau T, Blauth M, Lindsey RW, Donow C, Tscherne H. Recurrent rotational deformity of the femur after static locking of intramedullary nails: case reports. J Bone Joint Surg Br, 1997, 79: 4–8.
8. Braten M, Terjesen T, Rossvoll I. Torsional deformity after intramedullary nailing of femoral shaft fractures. Measurement of anteversion angles in 110 patients. J Bone Joint Surg Br, 1993, 75: 799–803.
9. Greenwood DC, Muir KR, Doherty M, Milner SA, Stevens M, Davis TR. Conservatively managed tibial shaft fractures in Nottingham, UK: are pain, osteoarthritis, and disability long-term complications? J Epidemiol Community Health, 1997, 51: 701–704.
10. Svoboda SJ, McHale CK, Belkoff SM, Cohen KS, Klemme WR. The effects of tibial malrotation on the biomechanics of the tibiotalar joint. Foot Ankle Int, 2002, 23: 102–106.
11. Wang X, Zhou Y, Shao H, Yang D, Huang Y, Duan F. Total knee arthroplasty in patients with prior femoral and tibial fractures: outcomes and risk factors for surgical site complications and reoperations. Orthop Surg, 2020, 12: 210–217.
12. Goodier WD, Calder PR. External fixation for the correction of adult post-traumatic deformities. Injury, 2019, 50: S36–S44.
13. Sarai T, Inoue T, Fujiwara K, Kuramoto K. Dynamic finite element analysis of impulsive stress waves propagating from distal end of femur. Acta Med Okayama, 2012, 66: 409–415.
14. McErlain DD, Milner JS, Ivanov TG, Jencikova-Celerin L, Pollmann SI, Holdsworth DW. Subchondral cysts create increased intra-osseous stress in early knee OA: a finite element analysis using simulated lesions. Bone, 2011, 48: 639–646.
15. Tsui CP, Tang CY, Leung CP, *et al*. Active finite element analysis of skeletal muscle–tendon complex during isometric, shortening and lengthening contraction. Biomed Mater Eng, 2004, 14: 271–279.
16. Kettelkamp DB, Hillberry BM, Murrish DE, Heck DA. Degenerative arthritis of the knee secondary to fracture malunion. Clin Orthop Relat Res, 1988, 245: 159–169.
17. Milner SA, Davis TR, Muir KR, Greenwood DC, Doherty M. Long-term outcome after tibial shaft fracture: is malunion important? J Bone Joint Surg Am, 2002, 84: 971–980.
18. van der Schoot DK, Den Outer AJ, Bode PJ, Obermann WR, van Vuqt AB. Degenerative changes at the knee and ankle related to malunion of tibial fractures. 15-year follow-up of 88 patients. J Bone Joint Surg Br, 1996, 78: 722–725.
19. Draper ER, Cable JM, Scanchez-Ballester J, Hunt N, Robinson JR, Strachan RK. Improvement in function after valgus bracing of the knee. An analysis of gait symmetry. J Bone Joint Surg Br, 2000, 82: 1001–1005.
20. Elahi S, Cahue S, Felson DT, Engelman L, Sharma L. The association between varus–valgus alignment and patellofemoral osteoarthritis. Arthritis Rheum, 2000, 43: 1874–1880.

21. Zhu Z, Wang L, Li D, *et al*. Motion analysis on patients with knee osteoarthritis merged with varus deformity. Sheng Wu Yi Xue Gong Cheng Xue Za Zhi, 2018, 35: 38–44.
22. Hamerman D. The biology of osteoarthritis. N Engl J Med, 1989, 18: 1322–1330.
23. Sharma L, Song J, Dunlop D, *et al*. Varus and valgus alignment and incident and progressive knee osteoarthritis. Ann Rheum Dis, 2010, 69: 1940–1945.
24. Sanders R, Anglen JO, Mark JB. Oblique osteotomy for the correction of tibial malunion. J Bone Joint Surg Am, 1995, 77: 240–246.
25. Ahmed AM, Burke DL. In-vitro measurement of static pressure distribution in synovial joints–part I: tibial surface of the knee. J Biomech Eng, 1983, 105: 216–225.
26. Riegger-Krugh C, Gerhart TN, Powers WR, Hayes WC. Tibiofemoral contact pressures in degenerative joint disease. Clin Orthop Relat Res, 1998, 348: 233–245.